

NASA Technical Memorandum 4803

# A Technique for Transient Thermal Testing of Thick Structures

Thomas J. Horn, W. Lance Richards, and Leslie Gong

July 1997



NASA Technical Memorandum 4803

# A Technique for Transient Thermal Testing of Thick Structures

Thomas J. Horn, W. Lance Richards, and Leslie Gong  
*Dryden Flight Research Center  
Edwards, California*



National Aeronautics and  
Space Administration  
Office of Management  
Scientific and Technical  
Information Program  
**1997**

# A technique for transient thermal testing of thick structures

Thomas J. Horn,<sup>\*</sup> W. Lance Richards,<sup>†</sup> and Leslie Gong<sup>‡</sup>

National Aeronautics and Space Administration  
Dryden Flight Research Center, MS 48202A, P. O. Box 273, Edwards, CA 93523

## ABSTRACT

A new open-loop heat flux control technique has been developed to conduct transient thermal testing of thick, thermally-conductive aerospace structures. This technique uses calibration of the radiant heater system power level as a function of heat flux, predicted aerodynamic heat flux, and the properties of an instrumented test article. An iterative process was used to generate open-loop heater power profiles prior to each transient thermal test. Differences between the measured and predicted surface temperatures were used to refine the heater power level command profiles through the iteration process. This iteration process has reduced the effects of environmental and test system design factors, which are normally compensated for by closed-loop temperature control, to acceptable levels. The final revised heater power profiles resulted in measured temperature time histories which deviated less than 25 °F from the predicted surface temperatures.

**Keywords:** structural tests, thermal testing, radiant heating, transient thermal simulation, heat flux, heat transfer

## NOMENCLATURE

|       |  |
|-------|--|
| $C_p$ | material specific heat, Btu/lb/°F  |
| DACS  | data acquisition and control system  |
| $dT$  | differential change in temperature, °F   |
| $dt$  | differential change in time, sec   |
| $du$  | differential change in internal energy, Btu  |
| FLL   | Flight Loads Laboratory at NASA Dryden Flight Research Center, Edwards, California |
| IR    | infrared   |
| LTA   | Lockheed Thermal Analyzer, Lockheed California Company, Burbank, California        |
| meas  | measured   |
| NASA  | National Aeronautics and Space Administration                                      |
| $P$   | power level  |
| PHYSX | Pegasus <sup>®</sup> Hypersonic Experiments project                                |
| pred  | predicted  |
| $q$   | heat flux, Btu/ft <sup>2</sup> /sec  |
| $t$   | time, sec  |
| $T$   | temperature, °F  |
| $u$   | internal energy, Btu   |
| $V$   | volume, in <sup>3</sup>  |
| $x$   | distance coordinate, in.   |
| X-15  | a hypersonic research aircraft project   |

---

<sup>\*</sup>Email: Tom.Horn@dfrc.nasa.gov; Telephone: (805) 258-2232.

<sup>†</sup>Email: Lance.Richards@dfrc.nasa.gov; Telephone: (805) 258-3562.

<sup>‡</sup>Email: Les.Gong@dfrc.nasa.gov; Telephone: (805) 258-3912.

|              |                                      |
|--------------|--------------------------------------|
| YF-12        | a prototype Mach 3 cruise aircraft   |
| $\Delta$     | finite change                        |
| $\rho$       | material density, lb/in <sup>3</sup> |
| $\tau$       | thickness, in.                       |
| $\tau^*$     | effective thickness, in.             |
| Superscripts |                                      |
| $s$          | specific point in time               |
| "            | per unit area                        |
| '''          | per unit volume                      |
| Subscripts   |                                      |
| $a$          | analytically predicted               |
| $m$          | measured                             |
| $n$          | iteration number                     |
| $q$          | per heat flux                        |

## 1. INTRODUCTION

Ground thermal testing is often required to establish the flight worthiness of, or conduct research on, structural components subjected to a thermally hostile flight environment. Steady-state tests may be used to simulate cruise flight conditions or to conduct research on a new structural concept at a particular temperature. Transient thermal tests are required if the structure is to be subjected to significant aerodynamic heating during the transient boost, re-entry phases of flight, or both. Such dynamic flight conditions generate thermal gradients in the structure, which only transient tests can accurately simulate.

Transient thermal tests have been conducted on a variety of aerospace vehicles, or their components, including the X-15 horizontal stabilizer,<sup>1</sup> YF-12 aircraft,<sup>2</sup> and Space Shuttle elevon seals.<sup>3</sup> These structures had thin skins or were thermally insulated, and a traditional closed-loop temperature control system was used to control surface temperature. Temperatures on these test articles were generally controlled to within  $\pm 15$  °F of the desired temperature profile.

A transient thermal test was recently conducted on the Pegasus<sup>®</sup> Hypersonic Experiment (PHYSX) wing glove.<sup>4</sup> The majority of the wing glove is a thin structure. However, the leading edge of the glove is relatively thick and the design of the glove requires that the temperatures on the leading edge be accurately simulated in order to introduce the proper thermal stresses into the structure. The existing closed-loop temperature control did not provide adequate control of the leading edge temperatures because the controlled temperature oscillated and diverged from the desired temperature profile. Therefore, a new open-loop heat flux control technique was developed for the transient thermal test of the PHYSX wing glove.

This paper describes the open-loop heat flux control technique that was developed for use on the leading edge of the PHYSX wing glove. Background information is provided on the facility, test systems, and test article used during the PHYSX test. A brief discussion of traditional feedback temperature control, as applied to transient thermal testing, and representative data are also presented. Experimental results obtained using the open-loop heat flux control method are discussed. The paper closes with discussion of recommended improvements of the open-loop heat flux control method. Note that use of trade names or names of manufacturers in this document does not constitute an official endorsement of such products or manufacturers, either expressed or implied, by the National Aeronautics and Space Administration.

## 2. BACKGROUND

The Flight Loads Laboratory (FLL, formerly known as the Flight Loads Research Facility,<sup>5</sup> and Thermostructures Research Facility,<sup>6</sup>) located at the National Aeronautics and Space Administration (NASA), Dryden Flight Research Center, Edwards, California is a facility specifically designed to perform combined thermal<sup>7</sup> and mechanical loading of aerospace structures.

---

<sup>®</sup>Pegasus is a registered trademark of Orbital Sciences Corporation, Fairfax, Virginia.

This section provides background information on: (1) the systems (including a thermal control system and radiant heater systems) used in the FLL for transient thermal testing of aerospace structures, (2) how transient temperature profiles are obtained, and (3) the PHYSX test article which sparked the development of the open-loop heat flux control method.

## 2.1 Thermal control

Temperature feedback control is used in many research and industrial applications. A wide variety of controllers are available with set point or multiple segment ramp and soak temperature control. However, the data acquisition and control system (DACS) in the FLL was specifically designed to perform a dynamic thermal simulation of a high-speed maneuvering aerospace vehicle. Figure 1 shows a schematic of this system, which was tailored to test thin wall structures, such as aircraft wing and fuselage sections. Temperature feedback control is implemented through an adaptive proportional integral algorithm.<sup>8</sup> Critical test article and heater dependent control parameters for the algorithm are obtained from a specimen identification test performed prior to the transient thermal test.

The FLL DACS is capable of controlling up to 512 zones. Each zone consists of a portion of the radiant heater which illuminates a certain area of the test article surface. A thermocouple is installed on the test article within each zone and is used as feedback to the control system. The DACS forces the temperature in each zone to follow a prescribed temperature time history (or profile). Each zone is assigned a profile which may change slope as often as once per second. Open-loop power commands may also be prescribed for all or part of the profile of a zone.

The electric power supplied to the radiant heaters is regulated by *zero-crossover* power controllers. This type of controller turns each cycle of 60-Hz alternating current on or off at the moment between cycles when the line voltage crosses zero (fig. 2). This control method minimizes electrical noise but causes pulsed heating that is especially evident at low power levels. The voltage and current supplied to the heater during each *on* cycle is set by the transformer which is feeding the power controller

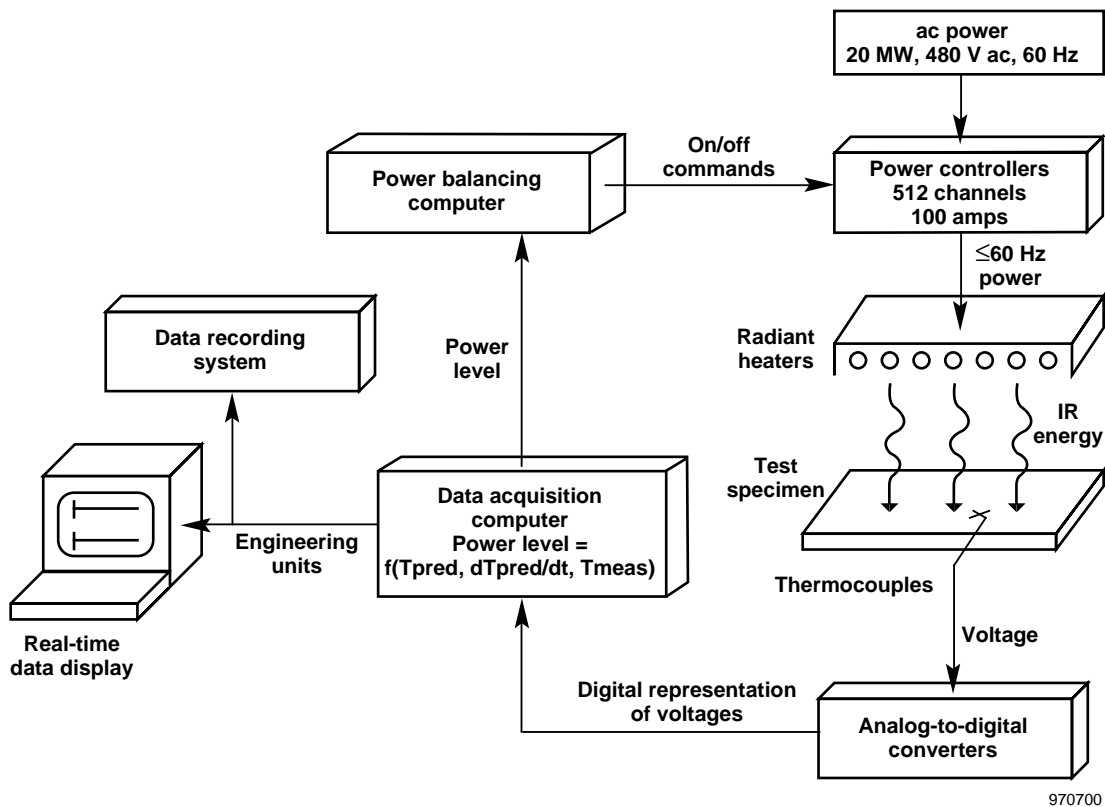


Figure 1. Feedback temperature control system in the Flight Loads Laboratory.

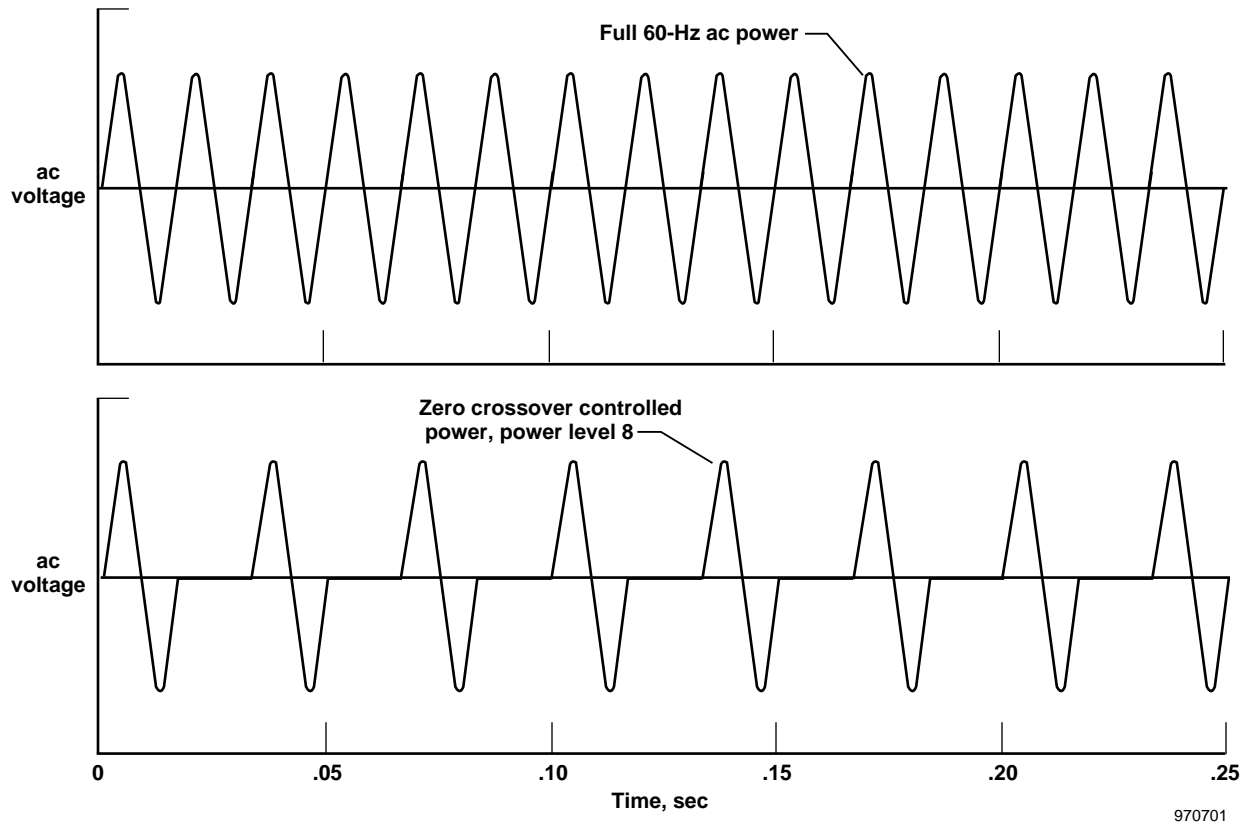


Figure 2. Zero-crossover power control.

and the electrical resistance of the radiant heater zone, not by the power controller itself. Zero-crossover power control is rarely a problem in closed-loop temperature control because the test article temperature rise caused by a single pulse is usually small.

The zero-crossover power control results in a discretized power level command. The DACS can adjust power level commands every 0.25 sec. Therefore, the DACS power commands are integer values which range from 0 to 15. These power levels correspond directly to the number of power cycles turned on in each 0.25-sec update interval.

## 2.2 Radiant heaters

The radiant heaters used in the FLL typically consist of three basic components: infra-red heat lamps, reflectors, and radiation fences. The heaters are custom built to the geometry and heating requirements of each test and may also accommodate other systems, such as test article instrumentation and cooling systems for the test article, the reflector, or both. Figure 3 shows the radiant heating system used in the PHYSX wing glove thermal ground test. The infrared heat lamps, often referred to as quartz lamps, are commercially available from major lamp manufacturers in a variety of wattages and lengths.

The reflectors are used to contain the radiant energy within the test system and direct as much energy as possible to the test article surface. These reflectors are manufactured from either fused silica ceramics or metals. Uncooled ceramic reflectors can operate for long periods of time at temperatures in excess of 2000 °F. Metallic reflectors (usually aluminum or stainless steel) are used uncooled for testing at low temperatures (<500 °F) and low heat flux (<10 Btu/ft<sup>2</sup>/sec). Water-cooled reflectors, air-cooled reflectors, or air- and water-cooled reflectors are used in tests requiring test article temperatures up to 3000 °F. These types of reflectors are also used in tests requiring heat fluxes as high as 100 Btu/ft<sup>2</sup>/sec.

Radiation fences are used at zone boundaries to minimize the influence of a zone on adjacent zones (i.e., crosstalk) and are typically made from fused silica ceramics. The ceramics offer several benefits including tolerance of temperatures up to

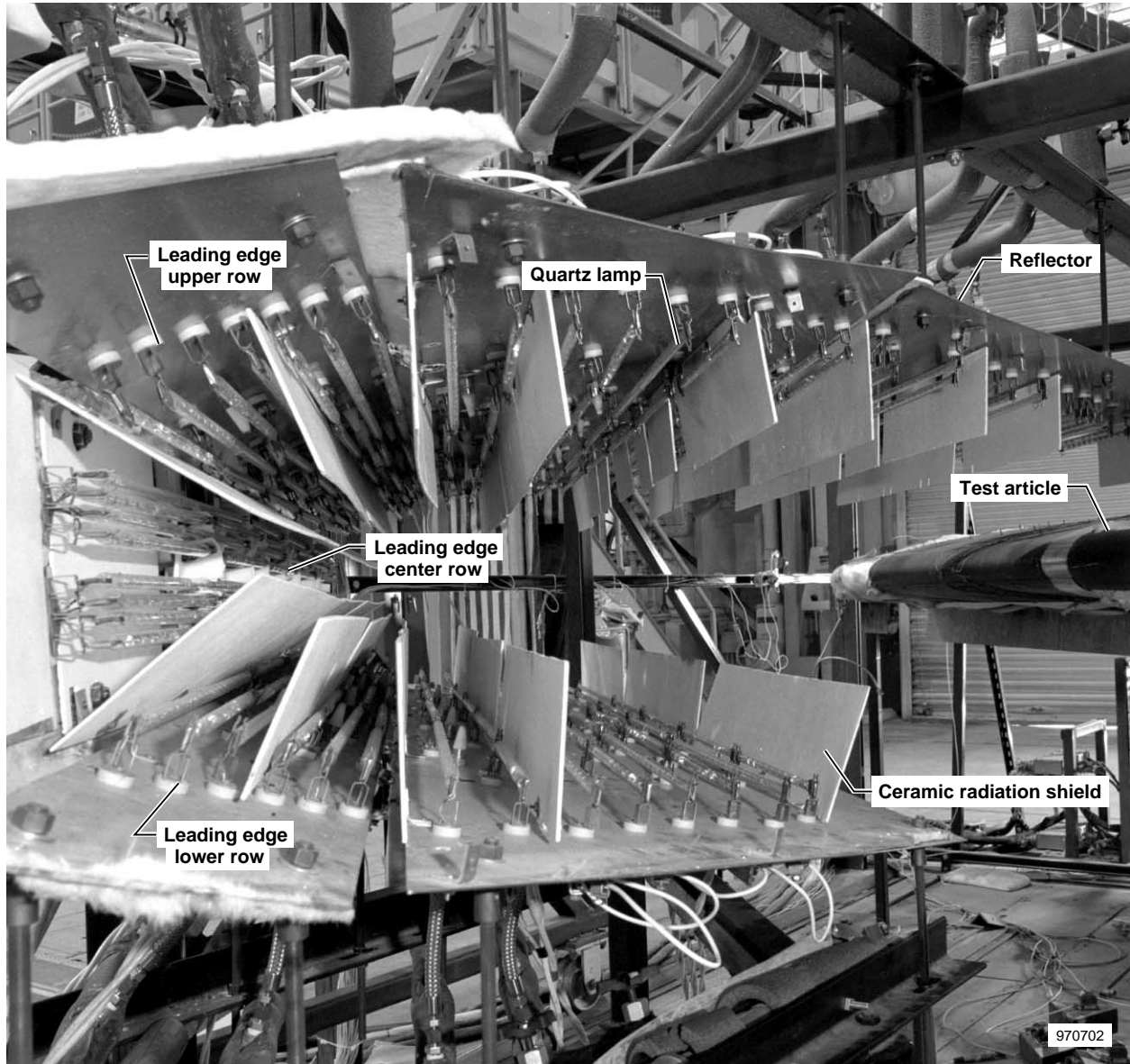


Figure 3. PHYSX wing glove radiant heating system, removed from test article.

3000 °F and minimal thermal expansion. Radiation fences are particularly critical when the heat fluxes being applied by adjacent zones are significantly different. The heater for the PHYSX wing glove (fig. 3) was designed with very narrow zones, approximately 1 in. wide, at the leading edge (left side of the figure) because the heat flux changes significantly from 27 Btu/ft<sup>2</sup>/sec at the leading edge (left-most lamps in the figure) to 6 Btu/ft<sup>2</sup>/sec two zones (about 4 in.) away.

### 2.3 Transient temperature profile generation

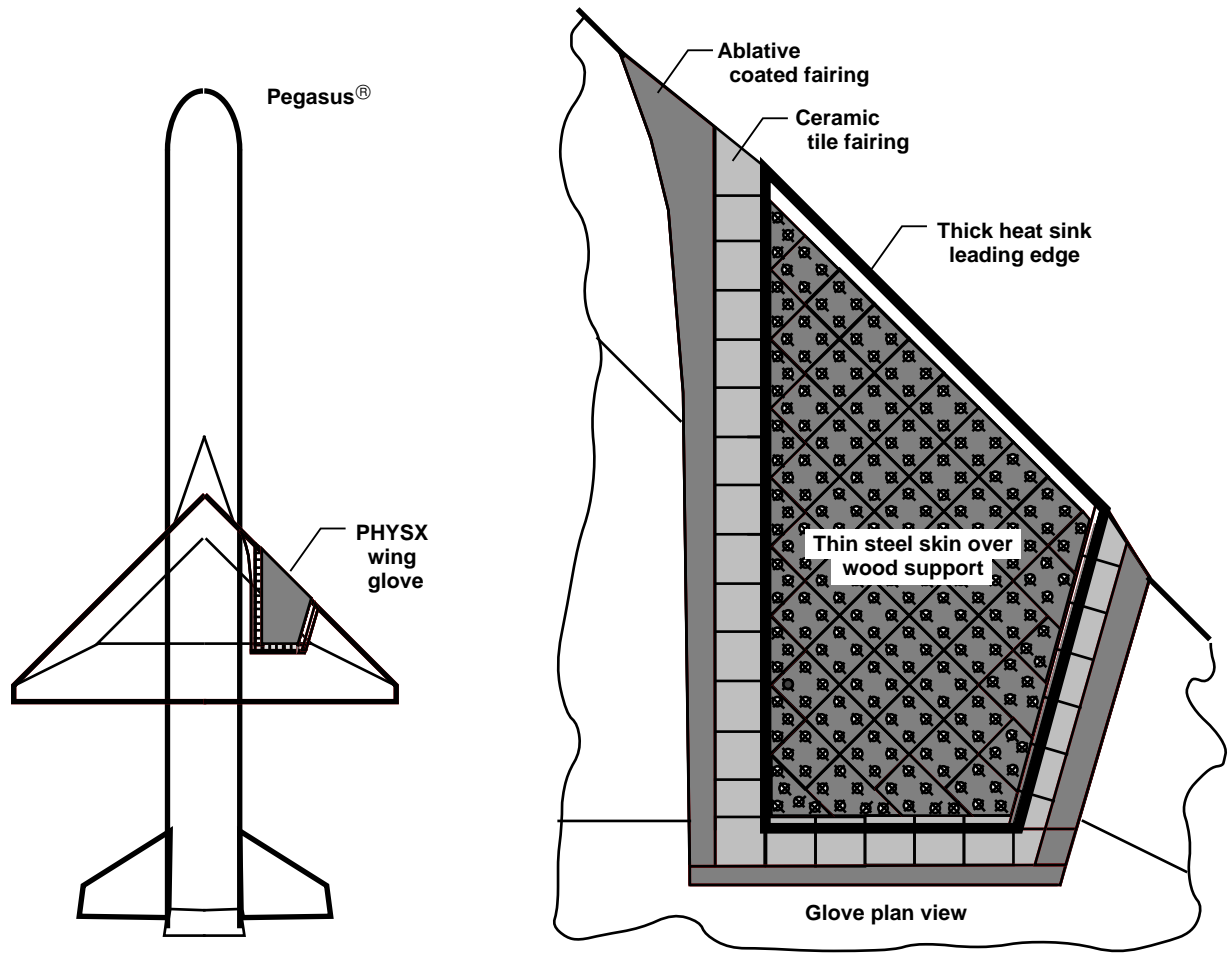
Transient temperature profiles may be obtained from either direct flight measurements or through an aerodynamic heating analysis. To begin the analysis, known flight time histories of altitude, Mach number, and angle of attack for the vehicle are used as input parameters for an aerodynamic heating program. The program then calculates transient time histories of surface temperatures, heating rates, heat transfer coefficients, skin friction, and surface static pressures for selected locations on the vehicle structure.

The transient aerodynamic heating program used at NASA Dryden is an in-house program called THEOSKIN. Each location on the vehicle structure is modeled by a single thermal mass, or lumped capacitance element. This model assumes a uniform temperature throughout the element although the actual structure may have a nonuniform temperature distribution. The thickness of the lumped capacitance element must be adjusted so that the element temperature in THEOSKIN represents the surface temperature of the real structure.

Finite-difference thermal models at various locations of interest on the vehicle structure are then developed using the Lockheed Thermal Analyzer<sup>9</sup> (LTA). The heating rates calculated by THEOSKIN are applied to the LTA thermal models that are used to calculate surface and structural temperature time histories. Peak surface temperature values obtained from LTA are compared to the peak temperature obtained from THEOSKIN for each location. If the temperature deviations are greater than a few degrees, the element thicknesses used in the THEOSKIN calculations are adjusted. After the element thicknesses are adjusted and new heating rates are calculated, the thermal models are executed again with the newer heating rates and the peak temperatures compared. This iterative process continues until the peak surface temperatures calculated in THEOSKIN are within a few degrees of the peak LTA surface temperature at each location. The predicted surface temperature time histories from LTA are then used as the required surface temperature control profiles.

### 2.4 PHYSX wing glove test article

The PHYSX wing glove<sup>4</sup> is a flight test article designed to gather hypersonic boundary-layer transition data at speeds up to Mach 8. The flight test article is mounted on the right wing of a Pegasus<sup>®</sup> air launched space booster (fig. 4). The glove is



970703

Figure 4. Plan view of Pegasus<sup>®</sup> booster and PHYSX wing glove.

manufactured from structural steel with the upper and lower surfaces being thin skins ( $\approx 0.1$  in. thick) and the leading edge being a thick (nominally 0.5 in.) structure in order to act as a heat sink. Numerous attachment fittings were machined into the leading edge, which more than doubled the local thickness of the part. The leading edge is rigidly attached to the upper and lower surface thin skins. The glove must maintain a prescribed shape during the Pegasus<sup>®</sup> first stage flight, beginning at an altitude of 38,000 ft and Mach 0.8 and progressing to an altitude of 200,000 ft and Mach 8 only 80 sec later. The launch temperature of the glove is  $-30$  °F. Temperatures on the leading edge reach 500 °F by the end of the 80-sec flight. The peak heat flux predicted on the glove ranges from 27 Btu/ft<sup>2</sup>/sec at the leading edge to 6 Btu/ft<sup>2</sup>/sec 4 in. behind the leading edge. The peak predicted heat flux at the trailing edge of the upper surface (48 in. behind the leading edge) is 3 Btu/ft<sup>2</sup>/sec.

A transient thermal ground test was required to validate the PHYSX wing glove design when exposed to the predicted aerodynamic heating environment. The thermal gradients on the surface and through the thickness of the leading edge are the primary causes of thermal stress in the wing glove. Therefore, accurate, real-time simulation of the leading-edge surface temperature time histories were required during the transient thermal test. A duplicate wing glove dedicated to the transient thermal test was manufactured and attached to a mock-up of the Pegasus<sup>®</sup> wing. The glove surface temperatures predicted by an aerodynamic heating analysis of the Pegasus<sup>®</sup> vehicle were to be imposed on the glove by the FLL radiant heating systems using closed-loop temperature control. Instrumentation on the test article included deflection potentiometers, strain gages, thermocouples, and heat flux gages. Deflection potentiometers, strain gages, and thermocouples were placed at various locations on the structure to obtain data for comparison to structural analyses. Thirty-nine thermocouples were placed on the exterior surface of the wing glove for use in feedback temperature control.

The heater for the PHYSX glove thermal test (fig. 3) was divided into 39 zones. The zones were grouped into rows with each row containing one to four zones, depending on the test article geometry and heating requirements. Each leading edge row had three roughly equal area zones. Figure 3 shows that the zones near the leading edge were smaller and had denser lamp spacing in order to apply the wide range of heating rates predicted for the leading edge.

A typical test began by precooling the test article to  $-30$  °F to simulate the cold soak condition at Pegasus<sup>®</sup> launch. This process generally took 45 minutes to 1 hour to complete, and resulted in significant frost buildup on the test article. Once the precooling process was complete and the glove attained a uniform  $-30$  °F temperature, the 80-sec transient thermal test was executed.

The FLL closed-loop temperature control system performed well on the thin skin areas of the glove (fig. 5). The control system accurately compensated for the presence of the frost buildup by increasing the power to the heaters as the frost removed heat from the test article by melting and boiling away. The closed-loop temperature control system generated temperatures within  $\pm 10$  °F of the desired profiles on the thin skins.

The closed-loop temperature control system did not provide adequate control in three rows which heated the leading edge structure because of the leading edge thickness and the heating rates being applied. These rows included 9 of the 39 control zones used in the test. The controlled temperature in the nine leading edge zones began to oscillate as the heating rate approached 5 °F/sec (fig. 6). As the heating rate exceeded 5 °F/sec, the oscillations increased to unacceptable levels. The deviations from the profile eventually exceeded limits, which caused an automatic shutdown of the heater system. This oscillating, diverging behavior was not an acceptable representation of the predicted flight profile. Because closed-loop temperature control was successful on the remaining 30 zones, this method was used to control them for the duration of the test program.

### 3. OPEN-LOOP HEAT FLUX CONTROL

An alternative to closed-loop temperature control for the leading edge upper, lower, and center rows of the heater is to directly control predicted absorbed heat flux at the surface of the test article. Unfortunately, the DACS thermal control software was optimized for closed-loop temperature control of thin skin test articles and could not be easily modified to use a closed-loop heat flux control algorithm.

Open-loop programming of the heater power levels was the only near-term alternative to temperature feedback control on the DACS. This would allow delivery of a prescribed incident heat flux profile but would not provide real-time compensation of changes in the absorbed heat flux caused by environmental factors. Therefore, the open-loop heat flux control method is necessarily an iterative process. It requires knowledge of the predicted and measured surface temperature profiles ( $T_a(t)$  and  $T_m(t)$ ),

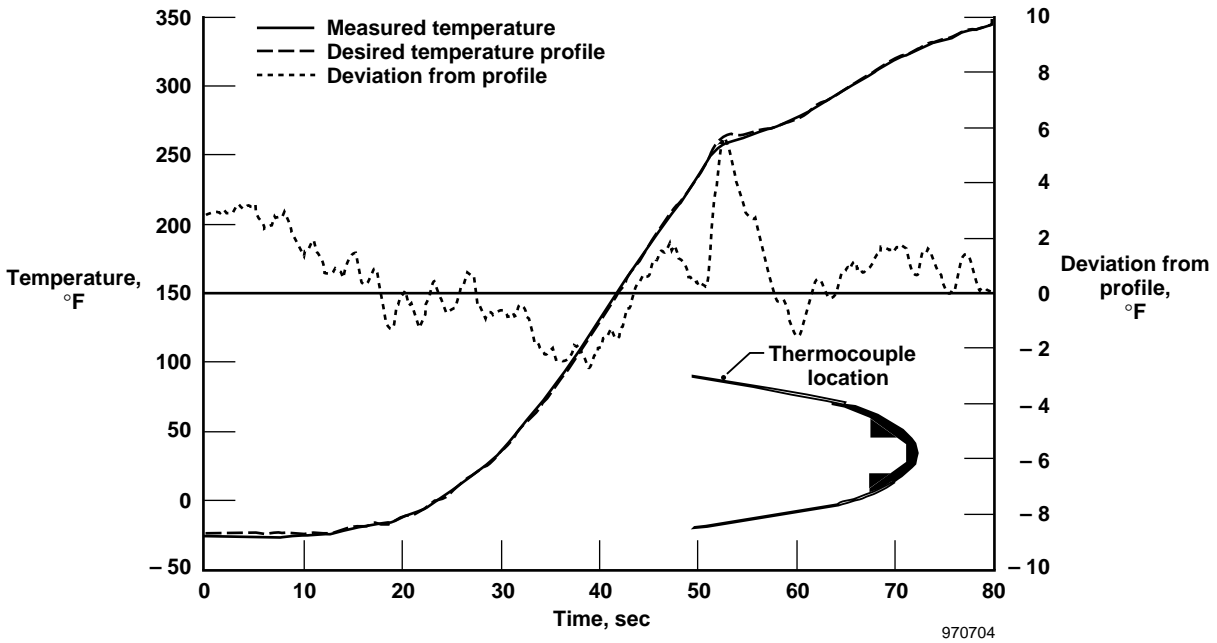


Figure 5. Temperature control of a thin skin zone.

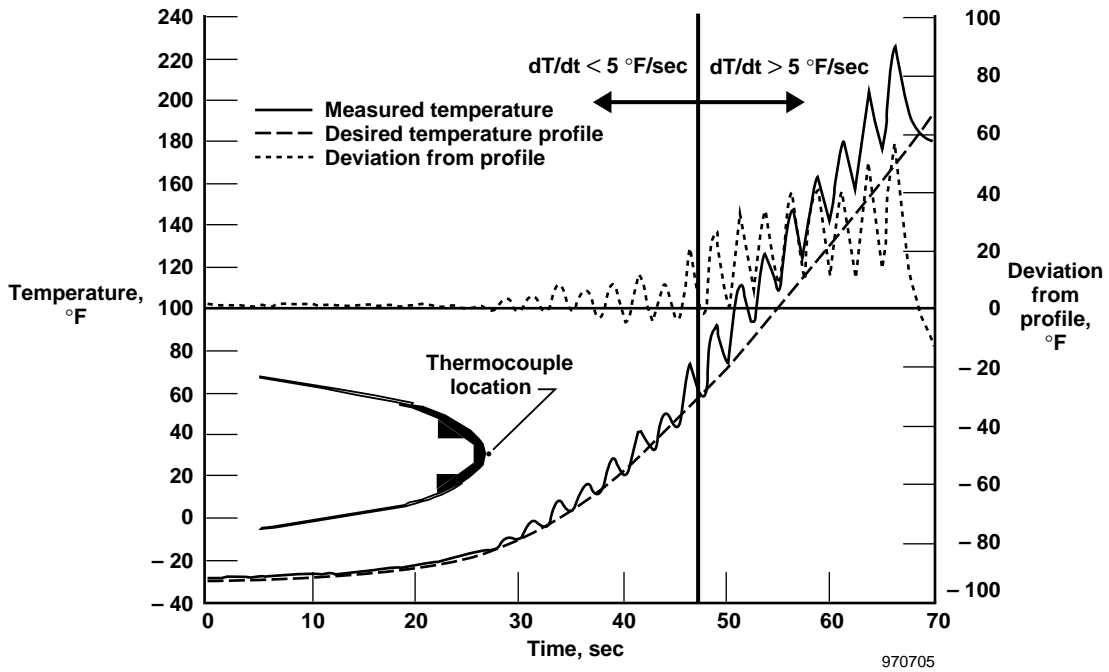


Figure 6. Temperature control of a leading edge zone.

the relationship between the heater power commanded and the absorbed heat flux obtained (represented by  $P_q$ ), the predicted absorbed heat flux profiles ( $q(t)$ ), and knowledge of the thermal properties of the test article, such as the density ( $\rho$ ), specific heat ( $C_p$ ), and surface thickness ( $\tau$ ).

### 3.1 Pretest activities

Figure 7 shows a flow chart summarizing the open-loop heat flux control technique described in this section. The process begins with the installation of calibrated heat flux gages on the surface of the test article. One heat flux gage was installed on the glove surface at the spanwise center of the leading edge upper, lower, and center rows (fig. 8) to directly measure the heat flux generated by the quartz-lamp heaters. It was assumed that the heat flux delivered at a given power level was constant along each row although each row consisted of three control zones. Therefore, only one heat flux gage was installed in the center zone of each row. Thermopile heat flux gages were installed in the leading edge upper and lower rows. A Gardon heat flux gage, capable of operating at temperatures in excess of 500 °F, was used in the leading edge center row. At this location, expected temperatures exceeded the capabilities of the thermopile heat flux gages available for use on the PHYSX wing glove test.

To apply the proper heat flux to the test article surface, the relationship between the heater power level commanded by the DACS and the heat flux actually produced by the heater was required. This relationship was assumed to be linear, based on past

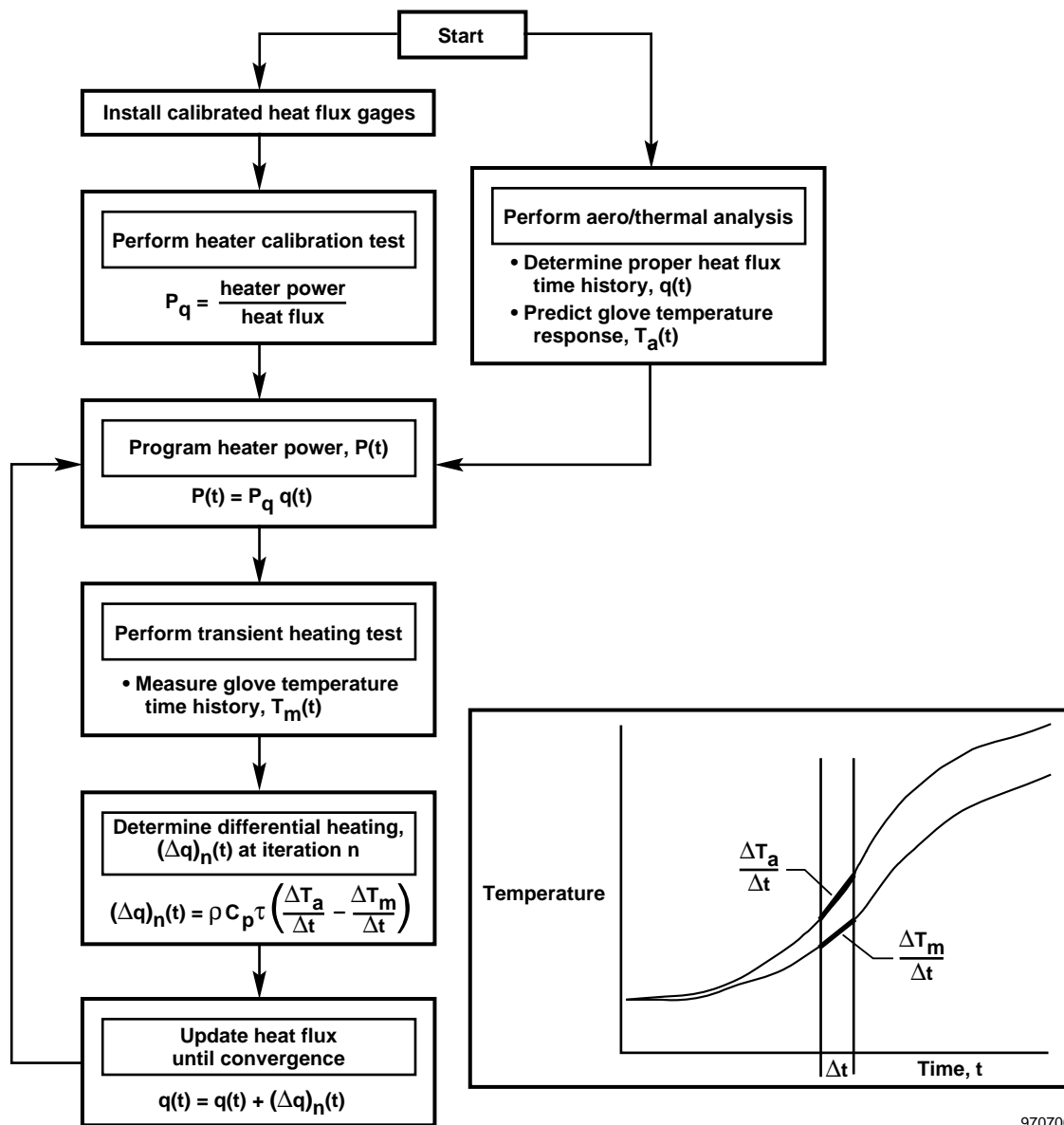


Figure 7. Open-loop heat flux control method.

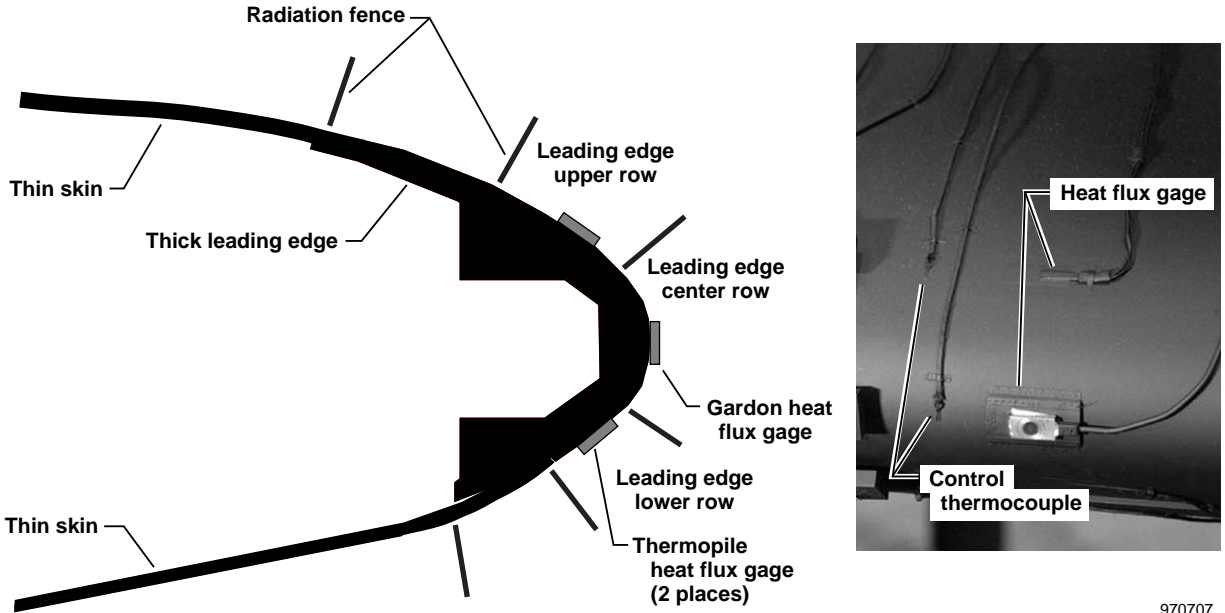


Figure 8. Heat flux gages on PHYSX wing glove.

experience in the FLL. The validity of this assumption is addressed in section 4.3. To obtain this relationship, a heater calibration test was performed at a constant power level. The level chosen was high enough to minimize the sawtooth heat flux profile caused by zero-crossover power control, yet low enough to limit temperatures and stresses in the glove to acceptable levels. Power level 5 met this requirement and was entered into the control computer. Each row of the heater was fired individually to obtain its power level per heat flux calibration ( $P_q$ ). Table 1 shows the calibration values obtained during the test. Crosstalk between the rows was less than 1 Btu/ft<sup>2</sup>/sec at power level 5 (fig. 9).

Table 1. Heater calibrations.

| Leading edge heater row | Heater calibration                      |
|-------------------------|---|
|                         | power level<br>Btu/ft <sup>2</sup> /sec |
| lower                   | 0.87                                    |
| center                  | 0.4                                     |
| upper                   | 0.91                                    |

The calibration test revealed significant temperature dependence in the output of the Gardon heat flux gage in the leading edge center row (fig. 9). The temperature dependence was observed as the heat flux gage temperature increased during the 10-sec application of a constant power level. The indicated heat flux dropped from 14 Btu/ft<sup>2</sup>/sec to 10.3 Btu/ft<sup>2</sup>/sec, although the power level (i.e. heat flux) was constant throughout the calibration test. Thermopile heat flux gages used in the upper and lower rows indicated a constant 1 Btu/ft<sup>2</sup>/sec while the center row was firing. The thermopile heat flux gages produced essentially constant heat flux measurements while their own rows fired as well. This confirms that the center row lamps emitted a constant heat flux and the indicated reduction in heat flux was a characteristic of the Gardon heat flux gage.

Another key step in the open-loop heat flux method is determining the heating rates required to accurately simulate the thermal environment. Aerodynamic heating rates calculated for each zone from the THEOSKIN program were used to determine the net heat flux profiles ( $q(t)$ ) required for open-loop heat flux control. Because these are the same heating rates used in determining the transient surface temperature time histories discussed in section 2.3, there was little additional effort required to generate these heat flux profiles.

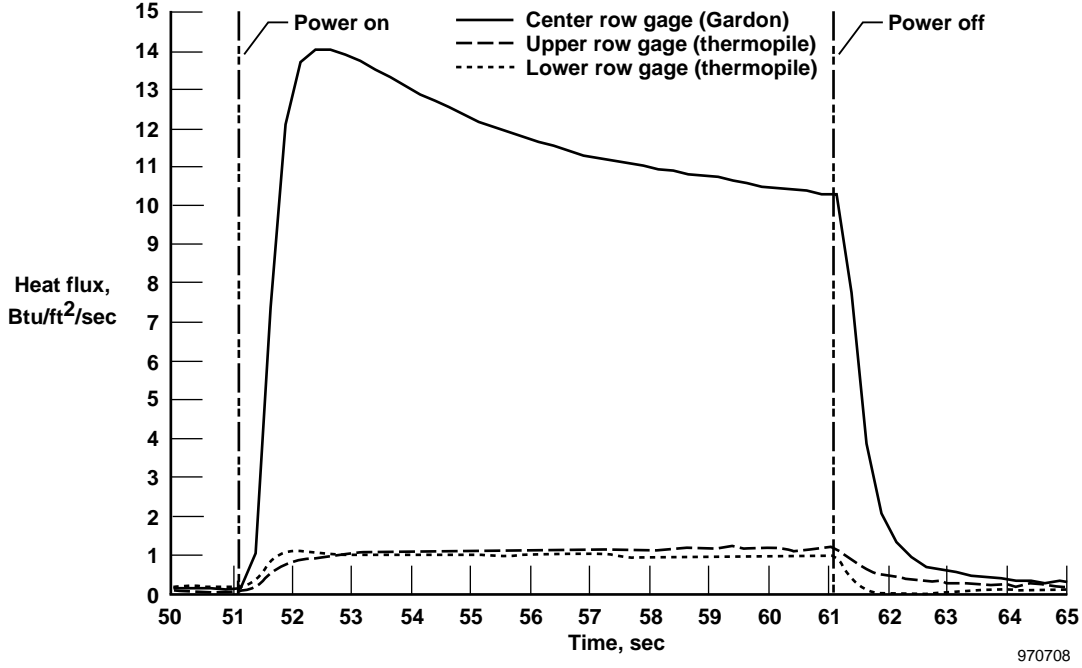


Figure 9. Measured heat flux during leading edge center row calibration test, center zone.

The heater power commanded by the DACS during the calibration test was divided by the actual heat flux obtained at the surface to obtain the heater calibration coefficient ( $P_q$ ) necessary for the control method. The heater power time histories were then generated by multiplying the predicted heat flux profile for a particular row by the heater calibration of that row.

$$P(t) = P_q q(t), \quad (1)$$

where  $P(t)$  is the power level programmed into the DACS, as a function of time. The crosstalk between the rows was not taken into account while generating power level profiles, because it was a relatively small component of the total heat flux being applied. An iteration process was used to account for all crosstalk as well as other environmental effects that were known to be present but were unpredictable.

### 3.2 Iteration process

After determining the necessary commands to the heaters, an initial test was performed and the transient temperature distributions at each zone on the glove were measured. Following the test, these measured temperatures ( $T_m(t)$ ), were compared to what was analytically predicted ( $T_a(t)$ ) for each second, and a differential heat flux profile for that time interval was calculated using the following equation (appendix A)

$$\Delta q_n(t) = \rho C_p \tau \left( \frac{\Delta T_a(t)}{\Delta t} - \frac{\Delta T_m(t)}{\Delta t} \right), \quad (2)$$

where  $\Delta q_n(t)$  = differential heat flux at iteration  $n$ , expressed as a function of profile time;  $\rho$  and  $C_p$  represent the density and the specific heat of the test article, respectively;  $\frac{\Delta T_a(t)}{\Delta t}$  and  $\frac{\Delta T_m(t)}{\Delta t}$  are the predicted and measured temperature rise rates at the heated surface of the test article, respectively; and  $\tau$  is the test article thickness. Note that equation (2) is based on a uniform temperature change per unit thickness. With thick structures subjected to transient heating, the temperature distribution through the thickness may not be constant. The full thickness of the test article at the leading edge center row ( $\tau = 0.5$  in.) was originally

used in equation (2). An effective thickness ( $\tau^*$ ) was then empirically determined based on a second test in order to increase the rate of convergence. The differential heat flux profile in equation (2) was then used to update heat flux profile,  $q_n(t)$ :

$$q_n(t) = q_{n-1}(t) + \Delta q_n(t), \quad (3)$$

This process was repeated until the procedure produced measured surface temperatures which matched the prescribed temperature profiles within the bounds of day-to-day variations ( $\approx 25$  °F), usually after the second or third iteration. Although not used in this test program, appendix B provides details as to how an effective thickness parameter ( $\tau^*$ ) can be analytically determined; depending on whether or not a back-sided temperature can be acquired during the test. Determining an accurate initial value of  $\tau^*$  using the analytical method proposed in appendix B may increase the convergence rate in the iteration process.

### 3.3 Limitations

The open-loop heat flux control method is not without its limitations and difficulties. Environmental influences, such as temperature, wind, and humidity, are difficult to account for because of their daily variations. Wind and temperature affected the PHYSX glove test because doors and vents in the FLL had to be open in order to remove nitrogen gas used to precool the glove. The precooling process also caused frost to build up on the PHYSX glove test article prior to the transient heating test. The frost accumulation increased the thermal mass to be heated and caused noticeable changes in glove surface temperature as the melted frost boiled off the glove. The wind and ambient temperature effects on the PHYSX glove were relatively small compared to the effect of frost buildup. However, the exact impact of any one environmental factor could not be determined because these factors could not be independently varied. Transient tests were run on consecutive days using the same temperature and power level profiles in order to quantify the overall impact of day-to-day environmental changes. The measured surface temperature time histories in a given open-loop zone differed by as much as 25 °F when the results of the two tests were compared. One should not expect the same open-loop profiles to deliver consistent results over a test program which lasts weeks, months, or longer, unless environmental factors can be well controlled.

The FLL test system itself presents a set of limitations which arise from the compromises that must be made during test system (both facility and test specific) design. In the FLL, zero-crossover power control results in a sawtooth heat flux profile at low power levels and discretized power command. The power commands in the FLL system are integer values which range from 0 (no firing) through 15 (fire all 15 alternating current cycles in the 0.25-sec control interval). Based on the heater calibration for the leading edge center row (0.4 power level/Btu/ft<sup>2</sup>/sec), the minimum change in heat flux available is 2.5 Btu/ft<sup>2</sup>/sec. This minimum change makes precise duplication of smoothly varying heat flux profiles, such as those predicted for the PHYSX wing glove, difficult.

Zone crosstalk is another difficulty caused by the test system. This difficulty might be eliminated in some special cases but generally all one can do is minimize zone crosstalk. The use of radiation fences and the iteration process can reduce this effect to acceptable levels.

The test article may also impose limits on the method. If the transient thermal test has a significant chance of damaging the test article or is planned as a test to failure, the ability to modify the open-loop profiles between tests may be limited. The iteration process was not used during the final 20 sec of the PHYSX glove heating profile because of a significant chance of damaging the test article during that time. A real-time modification of the open-loop heat flux control power level profiles or improved temperature feedback control would greatly reduce deviations from the desired profile during such *one-shot* tests.

The final difficulty with the method is heat flux sensor calibration uncertainty. One should expect large uncertainties in heat flux measurements given the current state of the art. The iteration process will eventually correct for this uncertainty, but a more accurate heat flux measurement leads to fewer iterations to converge on the desired temperature profile.

## 4. EXPERIMENTAL RESULTS AND DISCUSSION

Test data obtained on the open-loop heat flux control method can be grouped into three parts. First, data from a zone where a heat flux gage was installed will be discussed. Second, data from a zone that did not have a heat flux gage are presented to

highlight the ability of the iterative method to compensate for heater calibration errors. Finally, data are presented to validate the single power level calibration process.

#### 4.1 Zone with heat flux gage installed

Test data from a zone with a heat flux gage installed is shown in figure 10. Note that tests performed to support the iteration process were intentionally stopped at 60 sec to prevent possible damage to the test article. Once the iteration process converged in the first 60 sec, the full 80-sec test was run with no iteration performed between 60 and 80 sec. All tests began with the zone under temperature feedback control and switched to open-loop control at 12 sec. This allowed closed-loop temperature control to compensate for environmental effects at the beginning of the profile and provided a repeatable starting point for the open-loop portion of each profile. Temperatures within  $\pm 25$  °F of the desired profile were generated by the test performed after iteration, which is within the expected day-to-day variation caused by environmental factors. The fact that the measured temperature remained reasonably close to the predicted temperature profile after the 60-sec point indicates that the heater calibration used for this zone was accurate. In addition, environmental factors, such as frost, were the cause of the first test deviation from the desired profile.

#### 4.2 Zone without heat flux gage installed

The iteration process was particularly valuable in the open-loop controlled zones without heat flux gages. Errors in the assumed heater calibration can be large, because heat flux was not measured in these zones during the heater calibration test. Figure 11 shows the results obtained during transient testing. The measured temperatures were within the error band that was expected because of environmental effects. The deviation from the desired temperature grew after the 60-sec point when no iteration was possible. The open-loop heat flux control method provided an acceptable temperature profile even in zones where heat flux could not be directly measured.

#### 4.3 Heater calibration validation

The heater calibration calculation was performed for the leading edge center row using heat flux and power level data measured during the final transient thermal test (fig. 12). The original calibration was performed at a constant power level 5. Significant scatter and nonlinearity were noted in the data collected during the transient test below power level 5. Much of the

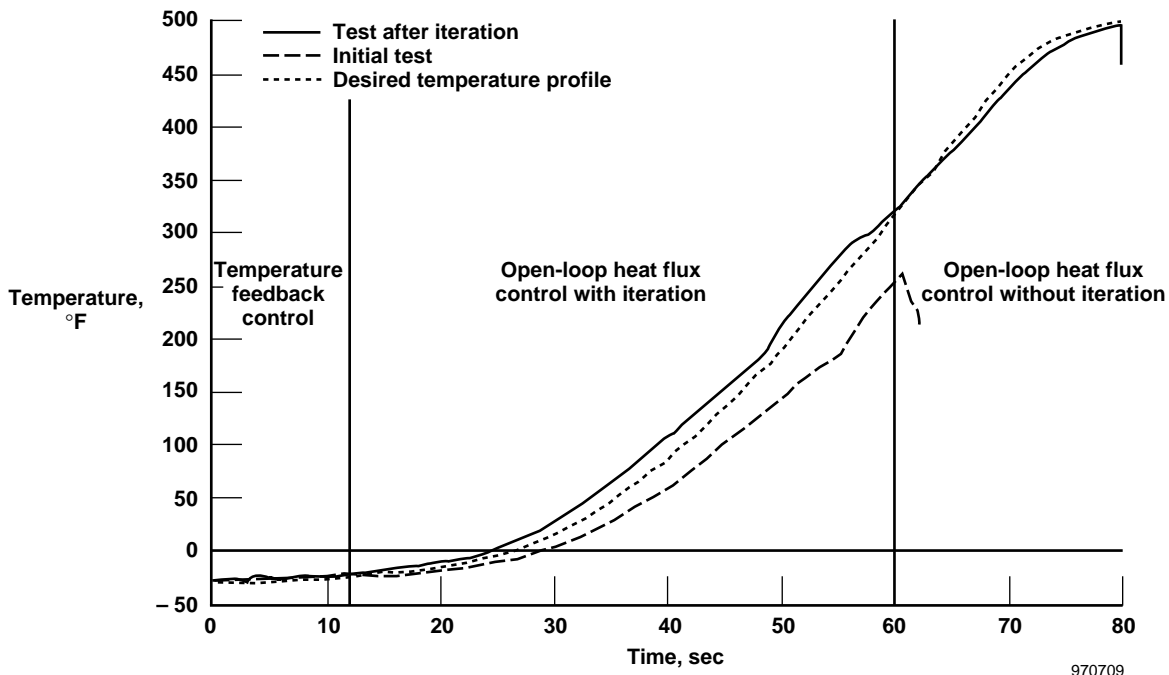


Figure 10. Results of open-loop process, zone with heat flux gage.

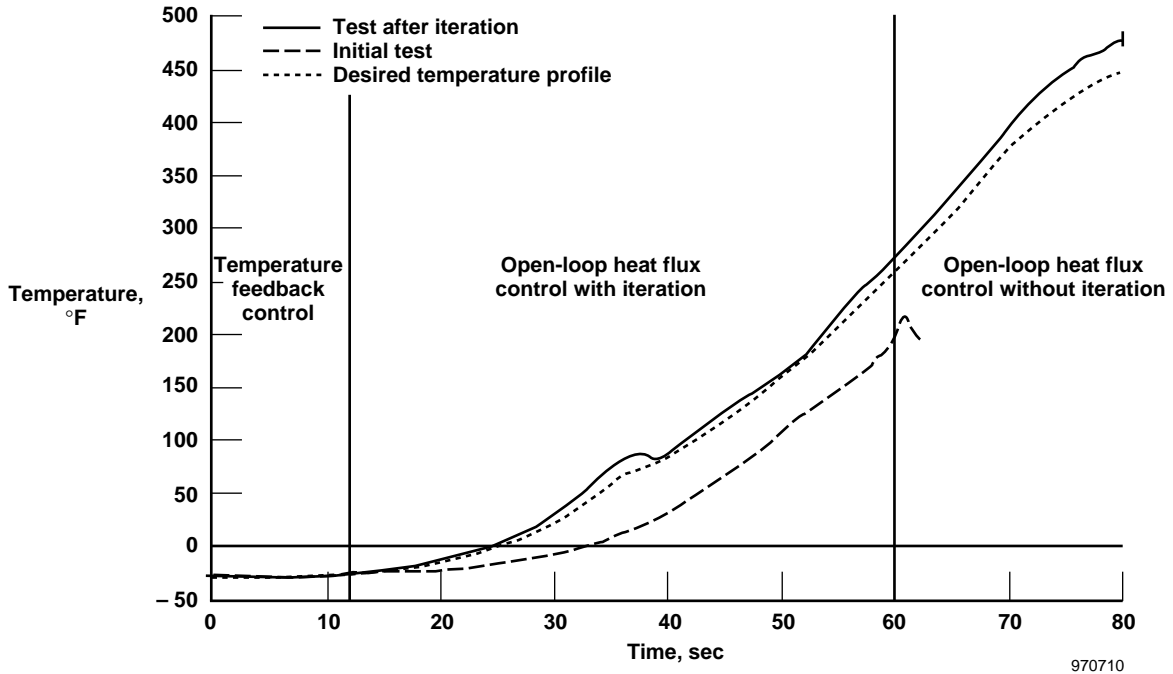


Figure 11. Results of open-loop process, zone without heat flux gage.

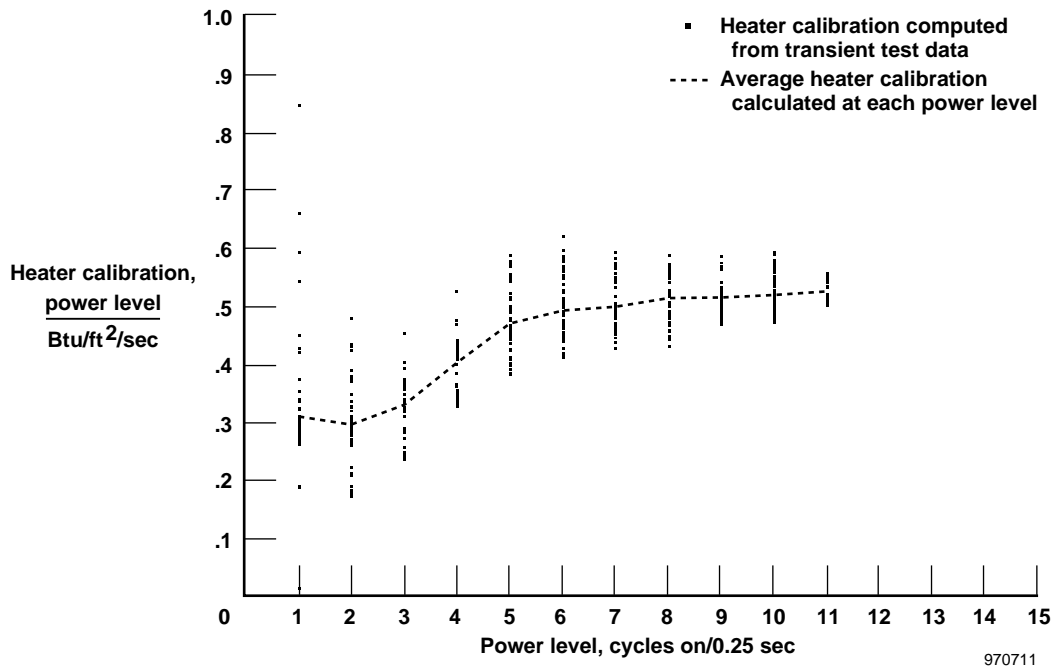


Figure 12. Heater calibration calculated from transient test data.

nonlinearity was caused by variation of the indicated heat flux with heat flux gage temperature (section 4.1). The scatter was caused primarily by the zero-crossover power control. The calibration calculation assumes that a constant heat flux value is generated at each power level, not the sawtooth pattern created by low power level zero-crossover control. A wide range of calibration values at low power levels results from the sawtooth heat flux pattern.

The transient heater calibration data taken above power level 5 shows that the linear assumption for the heater calibration is reasonable. The calibration in this power level range is nominally 0.5 power level/Btu/ft<sup>2</sup>/sec, somewhat above the calibration shown in table 1. This offset is due to the temperature-dependent output of the Gardon heat flux gage.

## 5. FUTURE WORK AND RECOMMENDATIONS

The method developed in this paper produced transient temperatures on the glove that were well within the program requirements. However, much of what was developed for the PHYSX represented a *work-around* solution given the time and budget constraints of the project, as well as limitations with the current data acquisition and control system used in the tests. The open-loop heat flux control technique was developed primarily because of a limitation with the current thermal control system in controlling the temperature of thick structures. Therefore, the first step for future work is to implement some of the lessons learned from this work into a new DACS. A new system with higher feedback rates in the control loop may improve the viability of temperature control of thick structures. Design and development of such a system is underway.

In many applications, temperature feedback control is not a viable option and the actual heat flux environment must be simulated. To this end, steps are currently being taken to program the algorithm developed in this paper into the next generation DACS so that adjustments to the heat flux profile can be made real time, instead of between tests. To avoid some of the limitations noted earlier with the present algorithm, other options are being explored to obtain accurate calculations of the differential heat flux.

Front and back surface temperature measurements should be made whenever possible during transient tests of thick structures. With such measurements, it is possible to integrate a one-dimensional finite-difference model in the iteration process. With this approach, the front and back surface temperatures measured during the test would be prescribed at boundary nodes of the model, and the nonlinear distribution through thickness of the surface would be calculated as well as an estimate of the absorbed surface heat flux. The differential heat flux required would be determined by subtracting the estimated surface heat flux from the absorbed heat flux predicted by the aerothermal analysis. With recent advancement in real-time processing, this process could be implemented real time instead of having to rely on posttest processing.

It will not always be possible to measure the back-side temperature of the test structure. In such a case, one must either assume an appropriate boundary condition at the back side of the structure in order to determine the absorbed heat flux analytically or make the constant temperature assumption. Reasonable values for  $\tau^*$  for use in equation (2) can be determined from a pretest thermal analysis as shown in appendix B.

## 6. CONCLUDING REMARKS

The new open-loop heat flux control technique that has been developed to conduct transient thermal testing of thick, thermally conductive aerospace structures uses calibration of the radiant heater system power level as a function of heat flux, predicted aerodynamic heat flux, and the properties of an instrumented test article. Open-loop heat flux control provides a reasonable alternative when the test article, test conditions, or both cause unstable temperature feedback control during transient thermal tests. Data from the Pegasus<sup>®</sup> Hypersonic Experiment (PHYSX) wing glove thermal test show that the method is successful in a challenging thermal test environment. Heat flux time histories and the heat flux per power level heater calibration must be determined prior to transient testing, in addition to the information usually required for temperature feedback control. Steady-state calibrations of the radiant heating system can be performed with sufficient accuracy to begin the iteration process. The iterative modification of the power level (i.e. heat flux) profiles is critical in order to account for various effects introduced by the environment, test systems, test article, and instrumentation.

Heat flux gages need not be installed in every zone if multiple zones can be expected to deliver similar heat flux to the test article. The assumptions made during the heater calibration test were confirmed by transient test data. The open-loop heat flux control method generated transient surface temperature histories within  $\pm 25$  °F of the desired profile on a thick, complex part exposed to large changes in applied heat flux over short distances. The iteration process was successful although a heat flux gage was installed in only the center zone of each spanwise row. The success of the open-loop heat flux control on the PHYSX wing glove warrants development of a real-time algorithm to provide increased accuracy during *one-shot* transient thermal tests.

## 7. APPENDIX A

Equation (2) was used to determine the change in heat flux ( $\Delta q$ ) necessary to ensure that the measured surface temperatures on the glove matched the desired temperatures predicted by the analysis. This appendix develops the mathematical basis for this equation.

When a structure of density ( $\rho$ ), volume ( $V$ ), and specific heat ( $C_p$ ) is heated transiently, such that the temperature increases by a differential change in temperature ( $dT$ ), the change in internal energy of the structure ( $du$ ) is given as

$$du = \rho V C_p dT(x, t) \quad (\text{A1})$$

where  $dT(x, t)$  represents the temperature difference between one-dimensional temperature distributions at a final and initial condition,  $x$  is a spatial dimension, and  $t$  is time. Dividing equation (A1) by the volume of the structure ( $V$ ) and integrating in the thickness direction ( $x$ ) from 0 to thickness  $\tau$ , the change in internal energy of a one-dimensional element with unit area is:

$$u'' = \int_0^{\tau} du''' dx = \int_0^{\tau} \rho C_p dT dx \quad (\text{A2})$$

where  $du'''$  represents the change in internal energy per unit volume. If all the terms on the right side of equation A2 are constant with respect to  $x$ , equation (A2) becomes

$$u'' = \rho C_p \tau dT \quad (\text{A3})$$

The heat transfer rate per unit area, or heat flux ( $q(t)$ ) can be determined simply by differentiating equation (A3) with respect to time,

$$q(t) = \rho C_p \tau \frac{dT}{dt} \quad (\text{A4})$$

Equation (A4) can now be employed to determine the surface heat flux as a function of time. This heat flux profile must be applied to produce a temperature time history ( $T(t)$ ) on the surface of the structure, provided that the temperature distribution through the thickness of the structure remains constant.

Figure A1 shows the case encountered with the initial testing of the PHYSX glove, in which the measured transient temperature at the heated surface ( $T_m(x=0, t)$ ) differed from a desired surface profile calculated analytically ( $T_a(x=0, t)$ ). The nomenclature in figure A1 is simplified with the following expressions:

$$T(t) = T(x=0, t) \quad (\text{A5a})$$

$$\Delta T^{(s+1)} = T(x=0, t=s+1) - T(x=0, t=s) \quad (\text{A5b})$$

$$\Delta t^{(s+1)} = t(s+1) - t(s) \quad (\text{A5c})$$

From figure A1, the net change in heat flux ( $\Delta q$ ) required in the time interval between  $s$  and  $s+1$ , ( $\Delta t^{(s+1)}$ ) to equate the two curves is

$$\Delta q(\Delta t^{(s+1)}) = \rho C_p \tau \left( \frac{\Delta T_a^{(s+1)}}{\Delta t^{(s+1)}} - \frac{\Delta T_m^{(s+1)}}{\Delta t^{(s+1)}} \right) \quad (\text{A6})$$



For the transient heating condition where the temperature distributions are not constant in  $x$ , as shown in figure B2, the change in internal energy in equation (A2) becomes:

$$u'' = \rho C_p \left[ \int_0^\tau \left( T_a^{(s+1)}(x) - T_m^{(s+1)}(x) \right) dx \right] \quad (B2)$$

Because equation (B1) is a specific case of equation (B2), the change in internal energy determined from the two equations will generally be different (fig. B2). The goal is to define an effective thickness parameter ( $\tau^*$ ) which, when multiplied by the surface temperature, will produce the same area as the shaded region in figure B2.

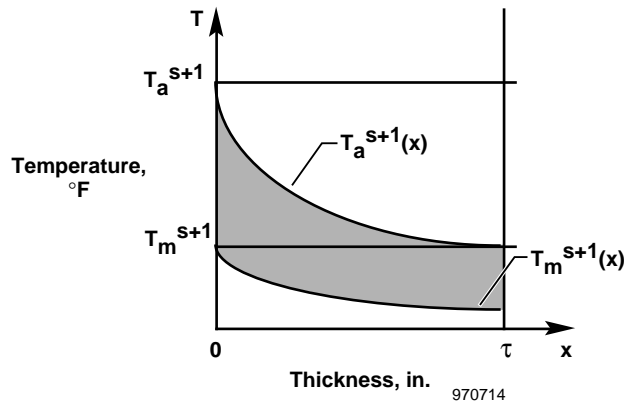


Figure B2.

Redefining  $\tau$  in equation (B1) as the effective thickness, ( $\tau^*$ ), setting equations (B1) and (B2) equal, and solving for  $\tau^*$ ,

$$\tau^* = \frac{\int_0^\tau \left( T_a^{(s+1)}(x) - T_m^{(s+1)}(x) \right) dx}{T_a^{(s+1)} - T_m^{(s+1)}}, \quad (B3)$$

which is shown graphically in figure B3.

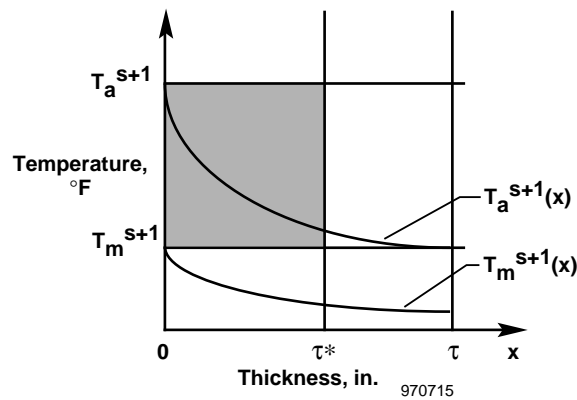


Figure B3.

Proper selection of  $\tau^*$  will improve convergence. Two methods are suggested to select an effective thickness. The first case is when both the front and back surface temperatures ( $T_m(0, t)$  and  $T_m(\tau, t)$ ) of the heated structure are measured during the transient thermal test. The second case is when only the front surface temperature of the structure is known. For the first case,  $T_a^{(s+1)}(x)$  can be determined at discrete nodal locations through the structure thickness using an aerothermal analysis, as described in section 2.3. If the front and back surface temperatures ( $T_m(0, t)$  and  $T_m(\tau, t)$ ) of the heated structure are measured during the transient thermal test, then these measurements can be prescribed as boundary conditions in an analysis, the interior temperature distribution, ( $T_m^{(s+1)}(x)$ ) can be determined analytically, and equation (B3) can be solved. Therefore, an appropriate thickness parameter is determined which ensures that the change in internal energy of the isothermally heated effective structure is equivalent to the change in internal energy produced by transient temperature distribution in the actual structure.

For the case where only the front surface temperature of the structures is known, further assumptions are in order. Assuming that the error between the desired and measured temperature profiles is caused by a greater uncertainty in the heat flux applied than in the material properties, and if the temperature distribution calculated from the test is reasonably close to the predicted values, then  $\tau^*$  can be approximated strictly based on the analytically determined temperatures. Replacing  $T_m^{(s+1)}(x)$  with  $T_a^{(s)}(x)$  in equation (B3) yields:

$$\tau^* = \frac{\int_0^{\tau} (T_a^{(s+1)}(x) - T_a^{(s)}(x)) dx}{T_a^{(s+1)} - T_a^{(s)}} \quad (\text{B4})$$

## REFERENCES

1. Fields, Roger A. and Andrew Vano, *Evaluation of an Infrared Heating Simulation of a Mach 4.63 Flight on an X-15 Horizontal Stabilizer*, NASA TN D-5403, Sept. 1969.
2. Olinger, Frank V., Walter J. Sefic, and Richard J. Rosecrans, "Laboratory Heating Tests of the Airplane," *NASA YF-12 Flight Loads Program*, NASA TM-X-3061, pp. 207–257, May 1974.
3. Fields, Roger A., *Flight Vehicle Thermal Testing with Infrared Lamps*, NASA TM-4336, Jan. 1992.
4. Richards, W. Lance and Richard C. Monaghan, *Analytical and Experimental Verification of a Flight Article for a Mach-8 Boundary-Layer Experiment*, NASA TM-4733, Mar. 1996.
5. Sefic, Walter J., *NASA Dryden Flight Loads Research Facility*, NASA TM-81368, Dec. 1981.
6. DeAngelis, V. Michael and Karl F. Anderson, *Thermal-Structural Test Facilities at NASA Dryden*, NASA TM-104249, Aug. 1992.
7. DeAngelis, V. Michael and Roger A. Fields, "Techniques for Hot Structures Testing," *Thermal Structures and Materials for High-Speed Flight*, Earl A. Thornton, Editor, vol. 140, AIAA, Washington D.C., 1992, pp. 255–277.
8. Zamanzadeh, Behzad, William F. Trover, and Karl F. Anderson, "DACS II - A Distributed Thermal/Mechanical Loads Data Acquisition and Control System," *International Telemetry Conference 1987, Instrument Society of America at San Diego, California*, Teledyne Controls, West Los Angeles, California, July 1987.
9. *Thermal Analyzer Computer Program for the Solution of General Heat Transfer Problems*, Lockheed California Company, LR 18902, July 1965.

# REPORT DOCUMENTATION PAGE

Form Approved  
OMB No. 0704-0188

Public reporting burden for this collection of information is estimated to average 1 hour per response, including the time for reviewing instructions, searching existing data sources, gathering and maintaining the data needed, and completing and reviewing the collection of information. Send comments regarding this burden estimate or any other aspect of this collection of information, including suggestions for reducing this burden, to Washington Headquarters Services, Directorate for Information Operations and Reports, 1215 Jefferson Davis Highway, Suite 1204, Arlington, VA 22202-4302, and to the Office of Management and Budget, Paperwork Reduction Project (0704-0188), Washington, DC 20503.

|   |   |   |  |
|---|---|---|--|
| <b>1. AGENCY USE ONLY (Leave blank)</b>   | <b>2. REPORT DATE</b><br>July 1997                              | <b>3. REPORT TYPE AND DATES COVERED</b><br>Technical Memorandum           |  |
| <b>4. TITLE AND SUBTITLE</b><br><br>A Technique for Transient Thermal Testing of Thick Structures   |   | <b>5. FUNDING NUMBERS</b><br><br>WU 529-60-24-00-17-00-DOC                |  |
| <b>6. AUTHOR(S)</b><br><br>Thomas J. Horn, W. Lance Richards, and Leslie Gong   |   |   |  |
| <b>7. PERFORMING ORGANIZATION NAME(S) AND ADDRESS(ES)</b><br><br>NASA Dryden Flight Research Center<br>P.O. Box 273<br>Edwards, California 93523-0273   |   | <b>8. PERFORMING ORGANIZATION REPORT NUMBER</b><br><br>H-2188             |  |
| <b>9. SPONSORING/MONITORING AGENCY NAME(S) AND ADDRESS(ES)</b><br><br>National Aeronautics and Space Administration<br>Washington, DC 20546-0001  |   | <b>10. SPONSORING/MONITORING AGENCY REPORT NUMBER</b><br><br>NASA TM-4803 |  |
| <b>11. SUPPLEMENTARY NOTES</b><br><br>Presented at the International Society for Optical Engineers Symposium, San Diego, California, July 27–August 1, 1997.  |   |   |  |
| <b>12a. DISTRIBUTION/AVAILABILITY STATEMENT</b><br><br>Unclassified—Unlimited<br>Subject Category 09  |   | <b>12b. DISTRIBUTION CODE</b>   |  |
| <b>13. ABSTRACT (Maximum 200 words)</b><br><br>A new open-loop heat flux control technique has been developed to conduct transient thermal testing of thick, thermally-conductive aerospace structures. This technique uses calibration of the radiant heater system power level as a function of heat flux, predicted aerodynamic heat flux, and the properties of an instrumented test article. An iterative process was used to generate open-loop heater power profiles prior to each transient thermal test. Differences between the measured and predicted surface temperatures were used to refine the heater power level command profiles through the iteration process. This iteration process has reduced the effects of environmental and test system design factors, which are normally compensated for by closed-loop temperature control, to acceptable levels. The final revised heater power profiles resulted in measured temperature time histories which deviated less than 25° F from the predicted surface temperatures. |   |   |  |
| <b>14. SUBJECT TERMS</b><br><br>Heat flux, Heat transfer, Radiant heating, Structural tests, Thermal testing, Transient thermal simulation  |   | <b>15. NUMBER OF PAGES</b><br>23  |  |
|   |   | <b>16. PRICE CODE</b><br>AO3  |  |
| <b>17. SECURITY CLASSIFICATION OF REPORT</b><br>Unclassified  | <b>18. SECURITY CLASSIFICATION OF THIS PAGE</b><br>Unclassified | <b>19. SECURITY CLASSIFICATION OF ABSTRACT</b><br>Unclassified            | <b>20. LIMITATION OF ABSTRACT</b><br>Unlimited |